MedChemComm

RESEARCH ARTICLE

View Article Online
View Journal | View Issue

Cite this: *Med. Chem. Commun.*, 2018, **9**, 1069

Pharmacophore-based tailoring of biphenyl amide derivatives as selective 5-hydroxytryptamine 2B receptor antagonists†

Moustafa T. Gabr *[ab] and Mohammed S. Abdel-Raziq[cd]

Received 16th April 2018,
Accepted 17th May 2018

DOI: 10.1039/c8md00204e

rsc.li/medchemcomm

We designed and synthesized a new biphenyl amide–tryptamine hybrid molecule **7** utilizing a pharmacophore-based approach as a 5-HT_{2B} antagonist. The hybrid compound **7** was evaluated for its affinity to a panel of seven 5-HT receptors, demonstrating high selectivity for the 5-HT_{2B} receptor. Functional assays revealed potent antagonism of 5-HT_{2B} by **7** with an IC_{50} value of 14.1 nM. Moreover, compound **7** possessed a desirable *in vitro* pharmacokinetic profile and maintained its antagonistic potency in the presence of physiological concentrations of serum proteins. The design approach implemented in this investigation would facilitate the development of a second generation of highly selective and potent 5-HT_{2B} antagonists.

Introduction

G protein-coupled receptors (GPCRs) represent the most prominent class of drug discovery targets owing to their key role in cell signalling events, and approximately one third of approved drugs rely on interactions with GPCRs.[1] The 5-hydroxytryptamine 2B (5-HT_{2B}) receptor, a member of the GPCR family, participates significantly in the regulation of cardiac function, gastrointestinal motility and CNS activity.[2] Consequently, selective 5-HT_{2B} antagonists have been explored as promising therapeutics for migraines, pulmonary arterial hypertension (PAH) and cardiac failure.[3–5] Additionally, recent studies showed that the 5-HT_{2B} receptor mediates the excitatory effects of serotonin in the human colon indicating that antagonists of this receptor might be valuable for the treatment of irritable bowel syndrome (IBS).[5]

Continuous research efforts have advanced several 5-HT_{2B} antagonists into clinical trials, however, there have been no 5-HT_{2B} antagonists clinically approved up to now.[6] This is mainly because of the insufficient selectivity displayed by reported 5-HT_{2B} antagonists against 5-HT_2 receptor subtypes.[7] In addition, the poor pharmacokinetic profiles of lead 5-HT_{2B} antagonists have hindered their clinical translational studies.[3a] We report herein a biphenyl amide–tryptamine hybrid scaffold as a selective 5-HT_{2B} antagonist utilizing a pharmacophore map of the recently identified structure of the 5-HT_{2B} receptor. Moreover, the likelihood of success of the hybrid scaffold is further investigated through *in vitro* pharmacokinetic profiling.

Rational design

GPCR structures display a common topology characterized by seven transmembrane (TM) helices interspersed with three intra-(ILs) and extracellular loops (ELs). The high degree of homology between the 5-HT_{2B} receptor and other relevant GPCR structures in the transmembrane (TM) segments has significantly limited the development of selective 5-HT_{2B} antagonists.[5a] Recent identification of the crystal structure of the 5-HT_{2B} receptor (PDB ID: 4IB4) has enabled structure-based design strategies seeking selective antagonists against this protein.[8] Taking into account the pronounced conformational changes of agonist-bound and antagonist-bound GPCR structures, a doxepin induced-fit model was recently introduced for the 5-HT_{2B} receptor which contributed to the discovery of triazine-based ligands as selective 5-HT_{2B} antagonists.[9] The triazine-based ligands occupy an orthosteric binding pocket in the 5-HT_{2B}–ergotamine complex without completely overlapping with the ergotamine binding site. The orthosteric binding site identified for 5-HT_{2B} antagonists based on the doxepin induced-fit model of the 5-HT_{2B} receptor (PDB ID: 4IB4) and the receptor-based pharmacophore map are shown in Fig. 1A and B, respectively. The required pharmacophoric features for binding include: (a) formation of a salt bridge interaction between a protonated amine

[a] *Department of Medicinal Chemistry, Faculty of Pharmacy, Mansoura University, Mansoura 35516, Egypt*
[b] *Department of Chemistry, University of Iowa, Iowa City, Iowa 52242, USA. E-mail: moustafatarekahmedibrahim-gabr@uiowa.edu; Tel: +1 3193599500*
[c] *Department of Pharmacognosy, Faculty of Pharmacy, Mansoura University, Mansoura 35516, Egypt*
[d] *School of Chemistry and Molecular Biosciences, University of Queensland, St Lucia 4072, Queensland, Australia*

† Electronic supplementary information (ESI) available. See DOI: 10.1039/c8md00204e

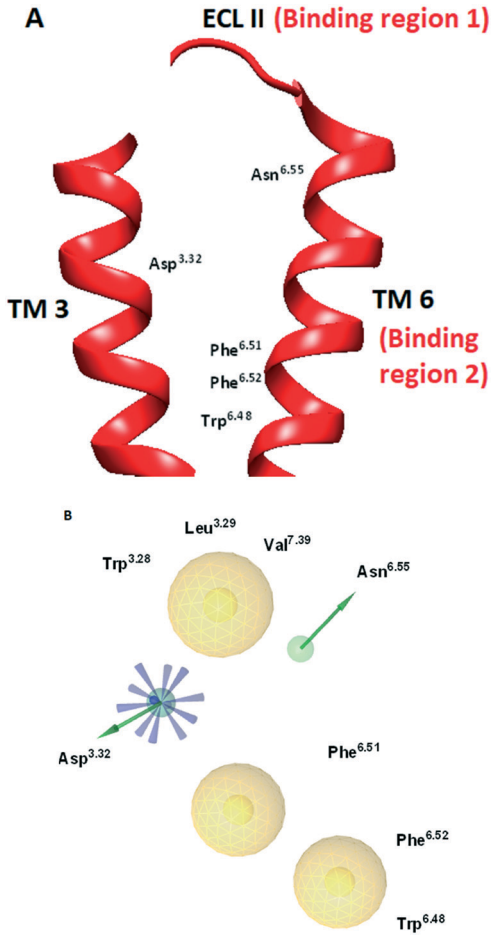

Fig. 1 (A) Orthosteric binding site for 5-HT_{2B} antagonists based on the doxepin induced-fit model of the 5-HT_{2B} receptor (PDB ID: 4IB4). (B) Receptor-based pharmacophore map generated for 5HT_{2B} antagonist interaction. The pharmacophore color coding is yellow for hydrophobic regions, blue for ionisable groups and green for hydrogen donors. TM: transmembrane; ECL: extracellular loop.

group in the ligand and an $Asp^{3.32}$ residue; (b) a hydrophobic group in the ligand that occupies the region of unfavourable water in the receptor; (c) additional hydrogen-bond formation with an $Asn^{6.55}$ residue of the binding pocket. The selectivity of this pharmacophore model arises from its ability to form additional hydrophobic interactions with binding region 1 near ECL II (Fig. 1A). The 5-HT_{2B} receptor is characterized by uniquely possessing three additional residues located in the ECL II region which enables the formation of the adjacent binding region 1 consisting of $Trp^{3.28}$, $Leu^{3.29}$ and $Val^{7.39}$ residues that other 5-HTRs lack. In addition, the ability to form an additional hydrogen bond with an $Asn^{6.55}$ residue of the receptor further contributes to the selectivity in comparison with other 5-HTRs lacking this residue (for example 5-HT_{1B}). Finally, the hydrophobic binding region 2 (Fig. 1A) consisting of $Phe^{6.51}$, $Phe^{6.52}$ and $Trp^{6.48}$ residues is identified in the generated pharmacophore map. Incorporation of sterically expansive groups into 5-HT_{2B} antagonists that are capable of exerting hydrophobic interactions with binding region 2 was found to be crucial for the antagonist activity.[9]

Compound **1** (Fig. 2) was identified as a lead 5-HT_{2B} antagonist from a high throughput screening campaign owing to its potent antagonism of the 5-HT_{2B} receptor[3a] which is comparable to the SmithKline antagonist SB215505 **2** (ref. 10) and the Roche antagonist RS-127445 **3** (ref. 11) (Fig. 2). Interestingly, compound **1** also displayed minimal activity against 5-HT_{2A} and 5-HT_{2C} receptors rendering it a valuable lead to achieve selective antagonism of 5-HT_{2B}.

In the current study, overlaying the pharmacophore of the lead compound **1** with the receptor-based pharmacophore (Fig. 1B) directed us to maintain the biphenyl amide fragment of **1** (Fig. 3) and further modify fragment B to achieve improved alignment to the receptor-based pharmacophore. To achieve this target, tryptamine was selected to replace fragment B of **1** as it is capable of hydrogen bonding to $Asp^{3.32}$ and $Asn^{6.55}$ residues which is crucial for potency and selectivity to the 5-HT_{2B} receptor. In addition, the tryptamine motif in the hybrid scaffold **7** would be an ideal fit to achieve the desired hydrophobic interactions at binding region 1 in ECL II of the target receptor (Fig. 1A). On the basis of the predicted binding mode, compound **8** was synthesized in which a tryptamine fragment is replaced with a benzyl group in order to elucidate the role of the tryptamine motif in binding the target receptor. Moreover, the effect of replacing the biphenyl group of fragment A in **7** with a phenyl ring was also studied *via* synthesizing the structural analogue **11** utilizing a similar synthetic approach.

Results and discussion

Pharmacophore analysis

3D and 2D pharmacophore maps were generated for compound **7** using LigandScout (Fig. 4). The investigated pharmacophoric features included hydrogen bond donors and acceptors as directed vectors, positive and negative ionizable regions and lipophilic areas that are represented by spheres. The pharmacophore scores listed in Table 1 were calculated for the alignment of the 3D pharmacophore of **7** and the receptor-based pharmacophore generated for the 5-HT_{2B} antagonists. Compound **7** displayed impressive alignment with the receptor-based pharmacophore with a pharmacophore score value of 92.1. The overlay of compound **7** with the receptor-based pharmacophore reveals the

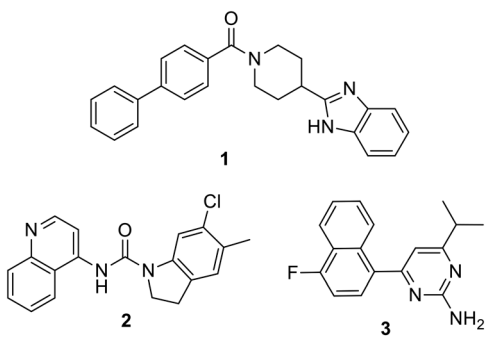

Fig. 2 Chemical structures of potent 5-HT_{2B} antagonists.

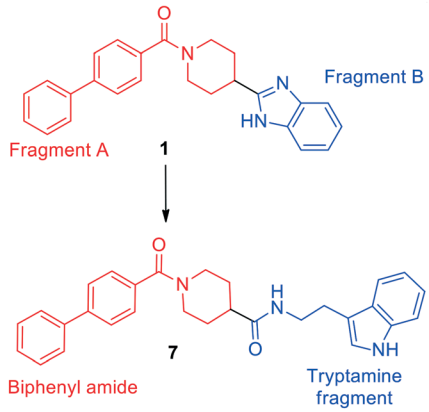

Fig. 3 Design strategy of biphenyl amide–tryptamine hybrid **7** based on the lead compound **1**.

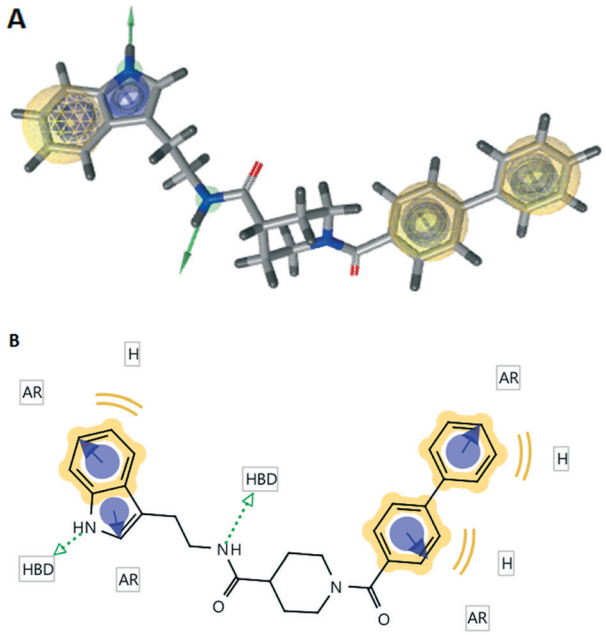

Fig. 4 The 3D and 2D pharmacophoric maps of compound **7**; (A) the 3D pharmacophoric map of compound **7**. The pharmacophore color coding is yellow for hydrophobic regions and green for hydrogen donors; (B) the 2D pharmacophoric map of compound **7**. H, hydrophobic center; HBD, hydrogen bond donor; AR, aryl.

Table 1 Pharmacophore scores of compounds **7**, **8** and **11**

Comp. no.	Pharmacophore score
1	65.9
7	92.1
8	14.5
11	76.4

comparable orientation of two hydrogen bond donors which are crucial for key interactions with the target receptor (ESI† Fig. S1). Moreover, the tryptamine fragment of compound **7** was overlaid with binding region 1 of the receptor pharmacophore map. The biphenyl moiety exhibited a satisfactory overlay with binding region 2. The 3D and 2D pharmacophore maps of the lead compound **1** (ESI† Fig. S2) displayed only one hydrogen bond donor and showed a pharmacophore score of 65.9 based on similarity to the receptor-based pharmacophore. It is worth mentioning that compounds **8** and **11** displayed pharmacophore scores of 14.5 and 76.4, respectively (Table 1).

Chemistry

The initial targets of this study were synthesized according to the approach outlined in Scheme 1. As shown in Scheme 1, the starting isonipecotic acid **4** reacted with biphenyl-4-carbonyl chloride **5** to afford compound **6** in serviceable yield. Further coupling of **6** with tryptamine and benzyl amine proceeded smoothly under microwave irradiation to furnish target compounds **7** and **8**. Similarly, compound **11** was synthesized *via* coupling of **9** (ref. 12) and tryptamine (Scheme 2).

Biological screening

Cellular functional assays were performed to validate the antagonist activity of the synthesized compounds against the 5-HT_{2B} receptor. To our delight, compound **7** displayed >95% inhibition of 5-HT_{2B} activity at 10 μM and 1 μM (Fig. 5A). Replacement of the tryptamine motif with a benzyl group in **8** completely eliminated the antagonist activity which validates our hypothesis of the pharmacophore-based design of tryptamine-based compounds. Replacing the biphenyl subunit with a phenyl group resulted in an ~10-fold decrease in potency (compound **11**). These results indicate that hydrophobic interactions exhibited by the biphenyl unit of **7** in binding region 2 of the receptor contribute significantly to the potency displayed by compound **7**. Further determination of the dose–response inhibition activity of compound **7** revealed that it exhibits an IC_{50} value of 14.1 nM (Fig. 5B).

To gain further insight into the selectivity of **7** against 5HT_{2B}, binding profiling tests were performed on a panel of 7 5-HT receptors (5-HT_{1A}, 5-HT_{1B}, 5-HT_{1E}, 5HT_{2A}, 5-HT_{2B}, 5-HT_{2C} and 5-HT_3). The results revealed that compound **7** is highly selective to the 5-HT_{2B} receptor (Table 2). Compound **7**

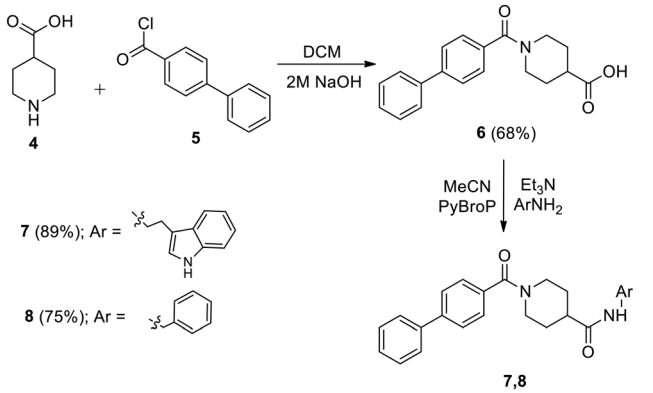

Scheme 1 Synthesis of compounds **7** and **8**.

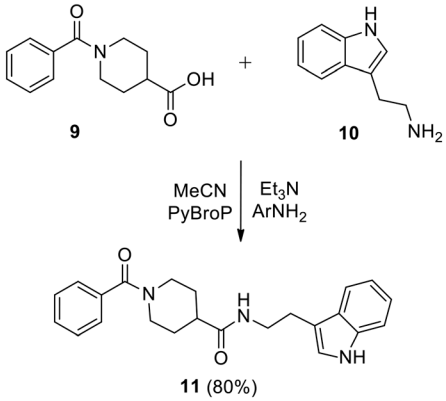

Scheme 2 Synthesis of compound **11**.

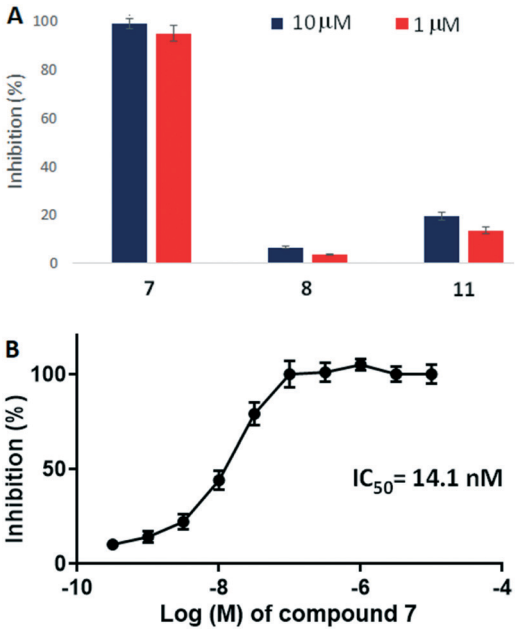

Fig. 5 (A) Inhibitory activities of **7**, **8** and **11** against the 5-HT$_{2B}$ receptor at 10 μM and 1 μM concentrations. (B) The dose-dependent inhibitory response curve of compound **7** with respect to the 5-HT$_{2B}$ receptor.

binds the 5-HT$_{2B}$ receptor tightly with a K_i value of 4.5 nM. However, **7** displays K_i values of 2460 and 473 nM against 5HT$_{2A}$ and 5-HT$_{2C}$, respectively, which are the two most highly related family members of 5-HT$_{2B}$. In addition, **7** displays generally weak binding against 5-HT$_{1B}$, 5-HT$_{1E}$ and 5-HT$_3$. Replacement of the tryptamine moiety with the benzyl group in **8** resulted in an ~130-fold decrease in binding affinity to the 5-HT$_{2B}$ receptor. Interestingly, compound **7** displayed >750-fold selectivity to 5HT$_{2B}$ over the closely related 5HT$_{1B}$ receptor in comparison to the ~15-fold selectivity of compound **8**. This significant difference in selectivity is attributed to the ability of the tryptamine moiety in **7** to form an additional hydrogen bond with the Asn$^{6.55}$ residue in the 5HT$_{2B}$ receptor. Moreover, the presence of the biphenyl moiety in **7** which is capable of interacting with ECL II region of 5HT$_{2B}$ resulted in ~11- and 8-fold improvements in selectivity over the 5HT$_{2C}$ and 5-HT$_{2A}$ receptors, respectively, in comparison with **11** possessing a phenyl group. These results are in good agreement with the proposed selectivity improvement to the 5HT$_{2B}$ receptor based on the pharmacophore-based design.

Pharmacokinetic profile

The ADME and toxicological parameters of the new biphenyl amide–tryptamine hybrid **7** were further examined (Table 3). The potencies of the benchmark 5-HT$_{2B}$ antagonists **2** and **3** drop by 50- and 27-fold, respectively, in the presence of 4% human serum albumin (HSA).[3a] In addition, the potency of the lead compound **1** drops by ~500-fold under similar conditions. Thus, there is a pressing need for the development of 5-HT$_{2B}$ antagonists that can maintain their potency in the presence of physiological concentrations of serum proteins. Interestingly, the potency of **7** was minimally affected in the presence of 4% HSA (Table 3) which is a distinguishing positive attribute of **7**. Compound **7** displayed high stability in simulated intestinal fluid of pH 6.5 and a relatively lower stability in gastric fluid of pH 1.6. Moreover, **7** demonstrated ~97% stability in human plasma over 2 h and was found to be relatively nontoxic to HepG2 liver cells. High permeability of **7** to CACO-2 cells was observed with no significant efflux (A to B P_{app} = 16.3 × 10^{-6} cm s^{-1}; efflux ratio = 2.01). The *in vitro* pharmacokinetic profile of **7** reveals its suitability for studying the role of 5-HT$_{2B}$ receptors.

Conclusions

In summary, a biphenyl amide–tryptamine hybrid scaffold **7** displayed selective and potent antagonism of the 5-HT$_{2B}$ receptor. The design strategy embraced structural tailoring of the potent 5-HT$_{2B}$ antagonist **1** to the receptor-based

Table 2 5-HTR binding profile results (K_i, nM)

Comp.	5-HT$_{1A}$	5-HT$_{1B}$	5-HT$_{1E}$	5-HT$_{2A}$	5-HT$_{2B}$	5-HT$_{2C}$	5-HT$_3$
7	603	3406	>10 000	2460	4.5	473	>10 000
8	9389	8594	>10 000	6794	569	986	>10 000
11	5396	7596	>10 000	5693	79.3	749	>10 000
Clozapine	Nd[a]	Nd	Nd	16.1	Nd	Nd	Nd
SB-206553	Nd	Nd	Nd	Nd	22.2	Nd	Nd
Ritanserin	Nd	Nd	Nd	Nd	Nd	1.9	Nd

[a] Nd; not determined.

Table 3 *In vitro* pharmacokinetic profile of **7**

Test	Comp. 7
Effect of HSA	
5-HT_{2B} IC_{50}	14.1
5-HT_{2B} IC_{50} + 4% HSA	18.7
Stability in simulated fluids ($t_{1/2}$, min)	
Gastric (pH 1.6)	259
Intestinal (pH 6.5)	>500
Stability in human plasma (% remaining at 120 min)	97.4
CACO cell permeability	
P_{app}, A → B (10^{-6} cm s^{-1})	16.3
P_{app}, B → A (10^{-6} cm s^{-1})	32.8
Stability in rat liver microsomes ($t_{1/2}$, min)	179
Cytotoxicity in HepG2 cells (IC_{50}, μM)	>50

pharmacophore map of the doxepin induced-fit model of the 5-HT_{2B} receptor. Additional exploration of the scaffold would furnish new tool compounds that should have great utility for mapping the binding surfaces of the 5-HT_{2B} receptor. Initial assessment of the *in vitro* pharmacokinetic profile of **7** suggests that it would serve as the foundation for the development of 5-HT_{2B} antagonists as potential therapeutics.

Experimental

General

All commercially available starting materials, reagents, and solvents were used as supplied, unless otherwise stated. The reported yields are isolated yields. Purification of all final products was accomplished by silica gel flash column chromatography. Chloroform : methanol or hexane : ethyl acetate was used as the elution solvent. Proton (^{1}H) and carbon (^{13}C) NMR were conducted on Bruker NMR spectrometers at 400 MHz for ^{1}H and 100 MHz for ^{13}C. Chemical shifts (δ) are reported in parts-per million (ppm) relative to the residual undeuterated solvent. Melting points were recorded using capillary melting point apparatus and are uncorrected. High resolution mass spectra were obtained using electron spray ionization (ESI†).

1-([1,1′-Biphenyl]-4-carbonyl)piperidine-4-carboxylic acid (6)

A suspension of biphenyl-4-carbonyl chloride **5** (10.83 g, 50.0 mmol) in dichloromethane (50 mL) was added to a solution of isonipecotic acid **4** (6.45 g, 50.0 mmol) in 2 M aqueous NaOH (50 mL). The reaction mixture was stirred for 8 h, then the reaction mixture was acidified using 1 M HCl and extracted with dichloromethane (3 × 50 mL). The combined organic layers were dried over anhydrous Na_2SO_4, filtered, and concentrated under reduced pressure. The crude product was purified by flash column chromatography using 10% ethyl acetate in hexane, followed by 60% ethyl acetate in hexane as the eluent to yield **6** (68%) as a white solid. Mp 115–117 °C. ^{1}H NMR (400 MHz, C*D*Cl_3) δ 1.83–1.86 (m, 2H), 2.07–2.11 (m, 2H), 2.66–2.73 (m, 2H), 3.18 (t, 2H, J = 10.6, 3.8 Hz), 3.84–3.97 (m, 1H), 4.55–4.61 (m, 1H), 7.43–7.54 (m, 5H), 7.64–7.70 (m, 4H), 9.89 (br s, 1H). ^{13}C NMR (100 MHz, $CDCl_3$) δ 28.0, 40.6, 45.2, 127.1, 127.2, 127.4, 127.8, 128.8, 134.3, 140.1, 142.7, 170.5, 179.0. HRMS (ESI): calcd for $C_{19}H_{18}NO_3$ $[M - H]^-$, 308.1286; found, 308.1291.

N-(2-(1*H*-Indol-3-yl)ethyl)-1-([1,1′-biphenyl]-4-carbonyl)-piperidine-4-carboxamide (7)

To a solution of compound **6** (310 mg, 1.0 mmol) in MeCN (4 mL), PyBroP (466 mg, 1.0 mmol) and Et_3N (0.32 mL, 2.5 mmol) were added and stirred at room temperature for 10 min. A solution of tryptamine (160 mg, 1.0 mmol) in MeCN (3 mL) was then added and the reaction mixture was stirred under microwave irradiation (80 W) at 90 °C for 20 min. The solvent was removed under reduced pressure, and the crude mixture was suspended in H_2O (20 mL) and extracted with dichloromethane (2 × 20 mL). The combined organic layers were dried over anhydrous Na_2SO_4, filtered, and concentrated under reduced pressure. The crude product was purified by flash column chromatography using 20% ethyl acetate in hexane, followed by 80% ethyl acetate in hexane as the eluent to yield **7** (89%) as a yellow-orange solid. Mp 160–162 °C. ^{1}H NMR (400 MHz, C*D*Cl_3) δ 1.51–1.76 (m, 4H), 2.62–2.89 (m, 6H), 3.42–3.51 (m, 2H), 3.64–3.67 (m, 1H), 4.52–4.57 (m, 1H), 6.21 (br s, 1H), 6.90 (s, 1H), 6.95–7.13 (m, 2H), 7.24–7.29 (m, 3H), 7.32–7.39 (m, 3H), 7.44–7.51 (m, 5H), 9.02 (s, 1H). ^{13}C NMR (100 MHz, C*D*Cl_3) δ 20.8, 24.8, 31.1, 36.2, 39.6, 42.4, 111.3, 112.1, 118.3, 118.9, 121.6, 122.3, 126.8, 126.9, 127.1, 127.3, 127.6, 128.7, 134.2, 136.3, 139.6, 142.4, 170.1, 174.3. HRMS (ESI): calcd for $C_{29}H_{30}N_3O_2$ $[M + H]^+$, 452.2338; found, 452.2336.

1-([1,1′-Biphenyl]-4-carbonyl)-*N*-benzylpiperidine-4-carboxamide (8)

Using the procedure given for the preparation of **7**, the coupling of **6** (310 mg, 1.0 mmol) and benzyl amine (107 mg, 1.0 mmol) gave **8** (75%) as a dark yellow solid after purification by flash column chromatography using 60% ethyl acetate in hexane as the eluent. Mp 132–134 °C. ^{1}H NMR (400 MHz, C*D*Cl_3) δ 1.75–1.95 (m, 4H), 2.41–2.47 (m, 1H), 2.82–2.98 (m, 2H), 3.86–3.99 (m, 1H), 4.43 (d, 2H, J = 5.7 Hz), 4.62–4.75 (m, 1H), 6.91 (t, 1H, J = 5.7, 5.7 Hz), 7.25–7.30 (m, 2H), 7.32–7.38 (m, 3H), 7.41–7.46 (m, 3H), 7.49–7.53 (m, 2H), 7.61–7.66 (m, 4H). ^{13}C NMR (100 MHz, C*D*Cl_3) δ 28.7, 41.7, 42.6, 43.1, 126.9, 127.0, 127.2, 127.4, 127.5, 127.7, 128.4, 128.7, 134.4, 138.3, 139.8, 142.3, 170.0, 173.9. HRMS (ESI): calcd for $C_{26}H_{27}N_2O_2$ $[M + H]^+$, 399.2072; found, 399.2073.

N-(2-(1*H*-Indol-3-yl)ethyl)-1-benzoylpiperidine-4-carboxamide (11)

Using the procedure given for the preparation of **7**, the coupling of **9** (233 mg, 1.0 mmol) and tryptamine (160 mg, 1.0 mmol) gave **11** (80%) as a yellowish orange solid after purification by flash column chromatography using 60% ethyl acetate in hexane as the eluent. Mp 155–156 °C. ^{1}H NMR (400 MHz, C*D*Cl_3) δ 1.54–1.81, 2.09–2.14 (m, 1H), 2.62–2.83 (m, 2H), 2.90–2.94 (m, 2H), 3.51 (d, 2H, J = 6.1 Hz), 3.61–3.64 (m,

1H), 4.57–4.62 (m, 1H), 6.55 (t, 1H, J = 5.6, 5.6 Hz), 6.87–6.89 (m, 1H), 7.04–7.15 (m, 2H), 7.21–7.24 (m, 2H), 7.28–7.36 (m, 4H), 7.56 (d, 1H, J = 7.6 Hz), 9.51 (s, 1H). ^{13}C NMR (100 MHz, C*D*Cl$_3$) δ 20.7, 24.8, 39.6, 42.2, 46.7, 111.2, 111.9, 118.1, 118.6, 121.3, 122.0, 126.2, 126.9, 128.2, 129.3, 135.4, 136.1, 170.1, 174.1. HRMS (ESI): calcd for $C_{23}H_{26}N_3O_2$ $[M + H]^+$, 376.2025; found, 376.2031.

Pharmacophore analysis

The crystal structure of the histamine H1–doxepin complex (PDB ID: 3RZE) was utilized to generate the initial binding mode of doxepin. The doxepin induced-fit model of the 5-HT$_{2B}$ receptor was prepared as reported previously[9] by overlaying the doxepin-bound GPCR structure with the 5-HT$_{2B}$ structure (PDB ID: 4IB4). The pharmacophore map of the binding mode was generated using LigandScout software, which was further used to generate the pharmacophore scores for the investigated compounds.

Biological assays

The CHO-K1/5-HT2B cell line was obtained from GenScript and used for cellular screening of the compounds. HepG2 cells were obtained from ATCC. Descriptions of the cellular function assay and binding assay are included in the ESI.† Briefly, cellular function assays were performed using the CHO-K1/5-HT$_{2B}$ cell line, using a calcium flux assay method. The binding assays were performed as previously reported.[13] Radiolabeled reference compounds ([^{3}H]8-OH-DPAT for 5-HT$_{1A}$; [^{3}H]GR127543 for 5-HT$_{1B}$; [^{3}H]5-HT for 5-HT$_{1E}$; [^{3}H] ketanserin for 5-HT$_{2A}$; [^{3}H]LSD for 5-HT$_{2B}$ and 5-HT$_{2C}$; [^{3}H] LY278584 for 5-HT$_3$) were used in the K_i determination assays. All assays were performed in triplicate.

In vitro pharmacokinetic assays

Descriptions of the assays are provided in the ESI† which were performed according to standard procedures.[14]

Conflicts of interest

The authors declare no competing interests.

Notes and references

1 (*a*) P. Nambi and N. Aiyar, *Assay Drug Dev. Technol.*, 2003, **1**, 305–310; (*b*) A. S. Hauser, M. M. Attwood, M. Rask-Andersen, H. B. Schioth and D. E. Gloriam, *Nat. Rev. Drug Discovery*, 2017, **16**, 829–842; (*c*) K. A. Jacobson, *Biochem. Pharmacol.*, 2015, **98**, 541–555; (*d*) D. Filmore, *Mod. Drug Discovery*, 2004, **7**, 24–28; (*e*) P. Kumari, E. Ghosh and A. K. Shukla, *Trends Mol. Med.*, 2015, **21**, 687–701.

2 (*a*) N. Kapadia, S. Ahmed and W. W. Harding, *Bioorg. Med. Chem. Lett.*, 2016, **26**, 3216–3219; (*b*) G. K. Shyu, *Circ. Res.*, 2009, **104**, 1–3; (*c*) S. Kantor, R. Jakus, B. Balogh, A. Benko and G. Bagdy, *Br. J. Pharmacol.*, 2004, **142**, 1332–1342; (*d*) S. Doly, E. Valjent, V. Setola, J. Callebert, D. Herve, J.-M. Launay and L. Maroteaux, *J. Neurosci.*, 2008, **28**, 2933–2940; (*e*) J.-M. Launay, B. Schneider, S. Loric, M. Da Prada and O. Kellermann, *FASEB J.*, 2006, **20**, 1843–1854; (*f*) M. M. Wouters, S. J. Gibbons, J. L. Roeder, M. Distad, Y. Ou, P. R. Strege, J. H. Szurszewski and G. Farrugia, *Gastroenterology*, 2007, **133**, 897–906; (*g*) F. Jaffre, J. Callebert, A. Sarre, N. Etienne, C. G. Nebigil, J.-M. Launay, L. Maroteaux and L. Monassier, *Circulation*, 2004, **110**, 969–974.

3 (*a*) N. Moss, Y. Choi, D. Cogan, A. Flegg, A. Kahrs, P. Loke, O. Meyn, R. Nagaraja, S. Napier, A. Parker, J. Thomas Peterson, P. Ramsden, C. Sarko, D. Skow, J. Tomlinson, H. Tye and M. Whitaker, *Bioorg. Med. Chem. Lett.*, 2009, **19**, 2206–2210; (*b*) A. Adegunsoye, M. Levy and O. Oyenuga, *BioMed Res. Int.*, 2015, **2015**, 929170.

4 (*a*) F. Jaffre, P. Bonnin, J. Callebert, H. Debbabi, V. Setola, S. Doly, L. Monassier, B. Mettauer, B. C. Blaxall, J. M. Launay and L. Maroteaux, *Circ. Res.*, 2009, **104**(1), 113–123; (*b*) B. Schaerlinger, P. Hickel, N. Etienne, L. Guesnier and L. Maroteaux, *Br. J. Pharmacol.*, 2003, **140**, 277–284; (*c*) J. M. Esteve, J.-M. Launay, O. Kellermann and L. Maroteaux, *Cell Biochem. Biophys.*, 2007, **47**, 33–44; (*d*) Y.-J. Liang, L.-P. Lai, B.-W. Wang, S.-J. Juang, C.-M. Chang, J.-G. Leu and K.-G. Shyu, *Cardiovasc. Res.*, 2006, **72**, 303–312.

5 (*a*) G. Poissonnet, J. G. Parmentier, J. A. Boutin and S. Goldstein, *Mini-Rev. Med. Chem.*, 2004, **4**(3), 325–330; (*b*) G. J. Sanger, *Trends Pharmacol. Sci.*, 2008, **29**, 465–471; (*c*) R. A. Borman, N. S. Tilford, D. W. Harmer, N. Day, E. S. Ellis, R. L. Sheldrick, J. Carey, R. A. Coleman and G. S. Baxter, *Br. J. Pharmacol.*, 2002, **135**, 1144–1151.

6 S. Ponnala, N. Kapadia and W. W. Harding, *Med. Chem. Commun.*, 2015, **6**, 601–605.

7 K. Ohashi-doi, D. Himaki, K. Nagao, M. Kawai, J. D. Gale, J. B. Furness and Y. Kurebayashi, *Neurogastroenterol. Motil.*, 2010, **22**, e69–e76.

8 D. Wacker, C. Wang, V. Katritch, G. W. Han, X. P. Huang, E. Vardy, J. D. McCorvy, Y. Jiang, M. Chu, F. Y. Siu, W. Liu, H. E. Xu, V. Cherezov, B. L. Roth and R. C. Stevens, *Science*, 2013, **340**, 615–619.

9 Y. Zhou, J. Ma, X. Lin, X.-P. Huang, K. Wu and N. Huang, *J. Med. Chem.*, 2016, **59**, 707–720.

10 C. Reavill, A. Kettle, V. Holland, G. Riley and T. P. Blackburn, *Br. J. Pharmacol.*, 1999, **126**, 572–574.

11 D. W. Bonhaus, L. A. Flippin, R. J. Greenhouse, S. Jaime, C. Rocha, M. Dawson, K. Van Natta, L. K. Chang, T. Pulido-Rios, A. Webber, E. Leung, R. M. Eglen and G. R. Martin, *Br. J. Pharmacol.*, 1999, **127**, 1075–1082.

12 S. Ventre, F. R. Petronijevic and D. W. C. MacMillan, *J. Am. Chem. Soc.*, 2015, **137**, 5654–5657.

13 J. Besnard, G. F. Ruda, V. Setola, K. Abecassis, R. M. Rodriguiz, X. P. Huang, S. Norval, M. F. Sassano, A. I. Shin, L. A. Webster, F. R. Simeons, L. Stojanovski, A. Prat, N. G. Seidah, D. B. Constam, G. R. Bickerton, K. D. Read, W. C. Wetsel, I. H. Gilbert, B. L. Roth and A. L. Hopkins, *Nature*, 2012, **492**, 215–220.

14 (*a*) D. K. Tosh, A. Finley, S. Paoletta, S. M. Moss, Z.-G. Gao, E. T. Gizewski, J. A. Auchampach, D. Salvemini and K. A.

Jacobson, *J. Med. Chem.*, 2014, **57**, 9901–9914; (*b*) J. L. Carlin, D. K. Tosh, C. Xiao, R. A. Pinol, Z. Chen, D. Salvemini, O. Gavrilova, K. A. Jacobson and M. L. Reitman, *J. Pharmacol. Exp. Ther.*, 2016, **356**, 475–483.